Manchester Metropolitan University

e-space

Manchester Metropolitan University's Research Repository

**Please cite the Published Version**

Sajid, Muhammad, Khan, Ali Haider, Malik, Tauqeer Safdar, Bilal, Anas, Ahmad, Zohaib and Sarwar, Raheem (2025) Enhancing Melanoma Diagnostic: Harnessing the Synergy of AI and CNNs for Groundbreaking Advances in Early Melanoma Detection and Treatment Strategies. International Journal of Imaging Systems and Technology, 35 (1). e70016 ISSN 0899-9457

**DOI:** https://doi.org/10.1002/ima.70016

**Publisher:** Wiley

**Version:** Published Version

**Downloaded from:** https://e-space.mmu.ac.uk/637702/

**Usage rights:** CC BY Creative Commons: Attribution 4.0

**Additional Information:** This is an open access article which first appeared in International Journal of Imaging Systems and Technology

**Data Access Statement:** Data sharing not applicable to this article as no datasets were generated or analysed during the current study.

**Enquiries:**
If you have questions about this document, contact openresearch@mmu.ac.uk. Please include the URL of the record in e-space. If you believe that your, or a third party's rights have been compromised through this document please see our Take Down policy (available from https://www.mmu.ac.uk/library/using-the-library/policies-and-guidelines)

*International Journal of Imaging Systems and Technology*

WILEY

RESEARCH ARTICLE OPEN ACCESS

# Enhancing Melanoma Diagnostic: Harnessing the Synergy of AI and CNNs for Groundbreaking Advances in Early Melanoma Detection and Treatment Strategies

Muhammad Sajid[1] | Ali Haider Khan[2,3] | Tauqeer Safdar Malik[4] | Anas Bilal[5,6] | Zohaib Ahmad[7] | Raheem Sarwar[8]

[1]Department of Computer Science, NFC Institute of Engineering & Technology, Multan, Pakistan | [2]Department of Software Engineering, Faculty of Computer Science, Lahore Garrison University, Lahore, Pakistan | [3]School of Software Engineering, Beijing University of Technology, Beijing, China | [4]Department of Information & Communication Technology, Bahauddin Zakariya University, Multan, Pakistan | [5]College of Information Science and Technology, Hainan Normal University, Haikou, China | [6]Key Laboratory of Data Science and Smart Education, Ministry of Education, Hainan Normal University, Haikou, China | [7]Department of Criminology and Forensic Sciences, Lahore Garrison University, Lahore, Pakistan | [8]OTEHM, Manchester Metropolitan University, Manchester, UK

**Correspondence:** Raheem Sarwar (r.sarwar@mmu.ac.uk)

**Received:** 4 May 2024 | **Revised:** 8 November 2024 | **Accepted:** 4 December 2024

**Funding:** The authors received no specific funding for this work.

**Keywords:** augmentation | cancer | deep learning; MCADT | dermoscopic medical image | health issue

## ABSTRACT

Skin cancer is one of the most prevalent and deadly neoplasms globally. Although melanoma constitutes a minor percentage of all skin cancer types, it presently stands as the primary cause of skin cancer-related deaths. Previous studies indicate that deep learning algorithms may identify subtle patterns and detailed features in medical images for melanoma detection, however, challenges remain due to the scarcity of annotated images and the intricacy of cancer images. The need for early skin cancer detection, particularly melanoma, is an urgent concern due to its potential for high mortality when not identified and treated promptly. This paper introduces a comprehensive method for melanoma detection in medical images through the incorporation of data augmentation approaches. We employed a CNN model for the categorization of melanoma images with data augmentation techniques such as random horizontal flips, random cropping, grayscale conversion, Gaussian blur, and random perspective transformations. Experiments demonstrate that the suggested method surpasses the existing peak performance in melanoma identification within medical imaging. The results indicate the potential of data augmentation techniques in alleviating the issue of insufficient medical images and improving melanoma detection. We attained an overall accuracy of 93.43%, a sensitivity of 99.74%, and a specificity of 88.53% in melanoma detection, surpassing state-of-the-art approaches with the HAM10000 dataset. Our model is beneficial in clinical settings to aid dermatologists in precisely identifying patients, facilitating early intervention, and potentially preserving lives. In the future, we intend to test our algorithm on more skin cancer datasets that may enhance the accuracy of melanoma diagnosis. A crucial component of the design is the ablation study, which seeks to discover and improve the most significant model parameters for computational efficiency and diagnostic precision. The HAM10000 dataset is utilized for ablation tests to assess and validate the efficacy of the suggested method.

This is an open access article under the terms of the Creative Commons Attribution License, which permits use, distribution and reproduction in any medium, provided the original work is properly cited.

© 2024 The Author(s). *International Journal of Imaging Systems and Technology* published by Wiley Periodicals LLC.

## 1 | Introduction

Skin lesions are prevalent, proliferative dermatological disorders that can be categorized as benign or malignant. Benign lesions generally exhibit moderate growth, lack metastasis, and do not impact adjacent or remote structures, often rendering therapy unnecessary [1]. Conversely, malignant tumors may spread and threaten adjacent tissues and organs, underscoring the necessity of early discovery and intervention for enhanced results. Artificial intelligence has facilitated computer-assisted diagnosis of skin diseases, presenting a viable method for accurate and efficient diagnostics [2]. In the forthcoming years, the global cancer burden will surely increase, presenting a significant threat to public health worldwide. The increasing proportion of adults and elderly patients are two critical elements leading to the escalation of cancer-related mortality. Moreover, although the prevalence of specific solid tumors has decreased in certain countries, the restricted efficacy of systemic treatments for various illnesses and contexts remains a significant issue [3]. Dermatologists can utilize AI systems to augment their clinical practice, integrating clinical data to boost the precision of AI-driven diagnosis [4, 5].

Changes in a lesion's dimensions, pruritus, and pigmentation may occasionally signify the onset of melanoma, as illustrated in Figure 1. Although non-melanoma skin cancers are more prevalent, melanoma is the most common cause of mortality. The likelihood of healing and survival markedly increases with the early discovery and identification of skin cancer. Considering the pivotal role of immunotherapy in cancer treatment, continuous investigation into factors that may affect treatment selection is essential [6]. Neglecting to do so may result in significant repercussions [7, 8]. African Americans, Asian Indians, Chinese Asians, and Africans have exhibited a consistent increase in melanoma prevalence over the past thirty years [9, 10]. Acral lentiginous melanoma (ALM) is the predominant kind of melanoma among individuals with darker skin in South Africa, often impacting the hands and feet [11]. Regrettably, the identification of melanoma is frequently postponed in those with darker skin, resulting in a poorer prognosis compared to those with lighter skin. Deep learning techniques have surfaced as the most promising methodology, exhibiting image-based diagnostic abilities akin to those of seasoned medical practitioners.

In a study [12], the scientists validated a CNN model using roughly 12 000 publically available dermoscopic images and discovered that the model surpassed 136 out of 157 clinicians in detecting malignant melanoma. Numerous deep learning models already yield probability scores for melanoma diagnosis; nevertheless, their opaque "black box" character raises questions regarding interpretability, which may mislead physicians. In response, numerous researchers have investigated CNN models that detect dermoscopic features and emulate the criteria employed for melanoma diagnosis, with the objective of generating better elucidative diagnostic outcomes through ensemble learning and transfer learning. Moreover, advanced techniques such as generative adversarial networks [13] and multi-task learning [14], coupled with enhanced data augmentation, have gained popularity in recent years. CNN models have markedly enhanced melanoma diagnosis when utilized with standardized, high-quality dermoscopic images. However, initiatives have been undertaken to integrate non-dermoscopic datasets, acknowledging the

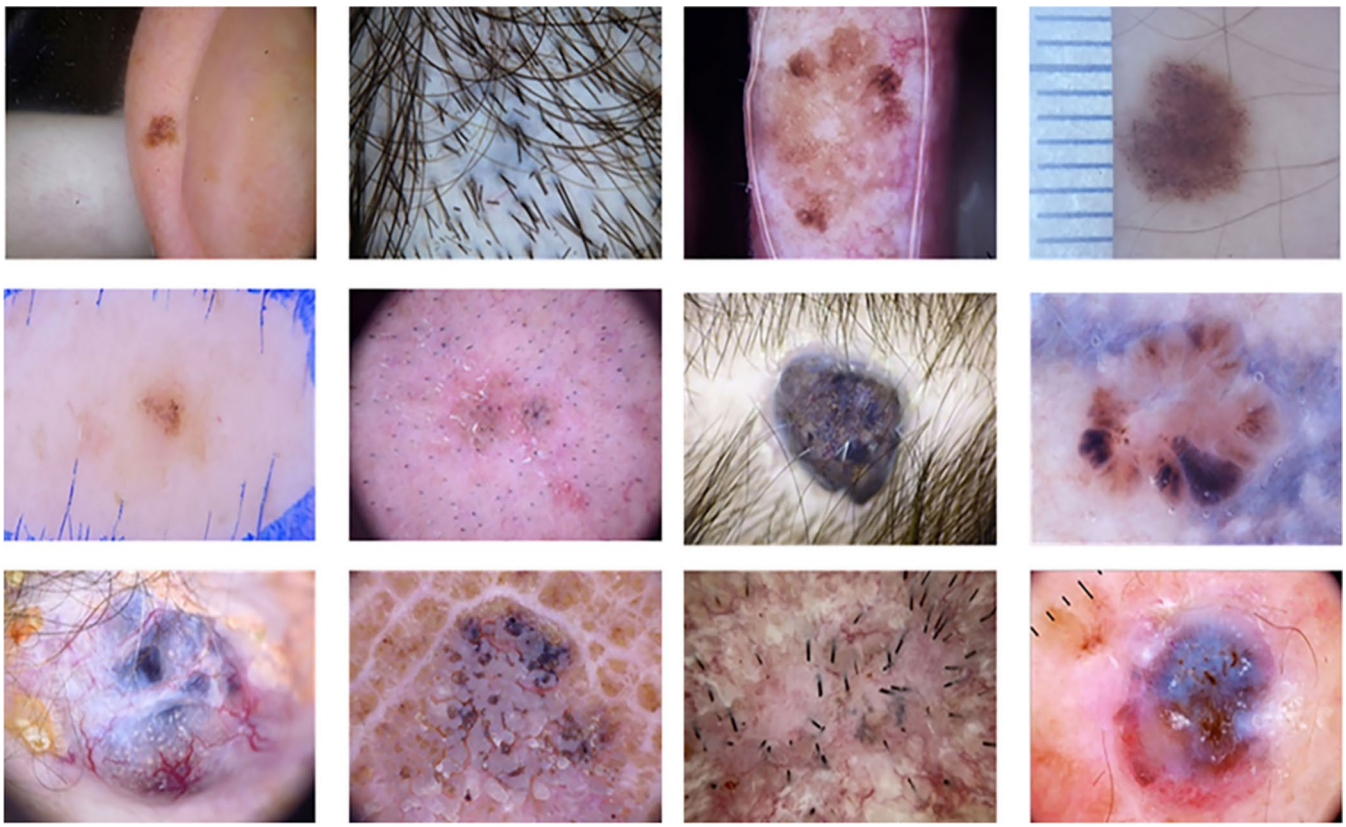

**FIGURE 1** | Different samples of dermoscopic medical images.

growing accessibility of images obtained with conventional digital cameras [15]. The inclusion of this extensive information seeks to promote the advancement of sophisticated and economical technologies [16–18].

The necessity for early identification of skin cancer, especially melanoma, is a pressing issue due to the potential for significant mortality if not recognized and treated swiftly. Manual evaluation by dermatologists results in inconsistencies in precision and postponements in prompt identification. Consequently, it is essential to create an automated model that utilizes Convolutional Neural Networks to analyze skin images and provide accurate melanoma identification. Our model would enable early intervention and can preserve lives. Despite breakthroughs in melanoma identification with convolutional neural networks, their accuracy is compromised by insufficient labeled data and the intrinsic complexity of melanoma images. We conducted research to further study the effectiveness to integrate augmentation techniques with CNN to improve the accuracy of melanoma diagnosis in response to the challenges presented. Our model MCADT effectively identifies skin lesions to protect individual health and enhance societal well-being. The main contributions of the study are outlined below:

1. To mitigate the dataset's shortage, we employed these five augmentation techniques RandomHorizontalFlip, RandomCrop, RandomPerspective, GaussianBlur, and Greyscale to enhance the medical image dataset.
2. We examine the efficacy of deep visual features derived from several pre-trained CNN models and assess their performance using a standard set of classifiers.
3. Our model MCADT assists dermatologists in precisely identifying patients, minimizing diagnostic errors, and ultimately enhancing patient outcomes.
4. We assess multiple potential combinations of CNN models and classifiers utilizing the benchmark dataset HAM10K.
5. We conduct ablation studies to illustrate the impact of numerous critical parameters, including preprocessing, optimizer, batch size, learning rate, number of epochs, and feature extraction at various CNN layers on our MCADT model.

## 2 | Related Work

Numerous studies have concentrated on creating a CAD strategy for skin cancer utilizing deep learning. This research followed the standard medical image analysis procedure [19], which includes image preparation, segmentation, feature extraction, and classification. Yet, current methodologies employing conventional image recognition techniques have demonstrated restricted efficacy, as they necessitate human feature estimate and extraction [20]. In contrast, convolutional neural networks can autonomously identify intricate nonlinear connections within images [12, 21]. This research [12] employed 4204 biopsy-validated pictures of melanoma and nevi (1:1) to train a convolutional neural network (CNN). Advanced deep learning techniques were integrated. In the study, an extra 804 biopsy-validated dermoscopic images of melanoma and nevi (1:1) were randomly shown to dermatologists from nine German university hospitals, who evaluated the quality of each image and offered their recommended treatments, amounting to a total of 19 296 recommendations. Three McNemar's tests were conducted to compare the CNN's test run results for sensitivity, specificity, and overall accuracy as the major outcomes. Automated dermoscopic melanoma image categorization demonstrated substantial superiority over both junior and board-certified dermatologists. Advanced research on skin cancer is now feasible. Recent research efforts have utilized deep learning algorithms to diagnose melanoma.

The authors of a study [21] provide a fresh dataset of clinical images obtained by cellphones, accompanied with relevant clinical data concerning patients, designated as the PAD dataset. The authors utilized pre-trained models derived from convolutional neural networks (CNNs). They subsequently propose a straightforward technique that employs an aggregation mechanism within existing deep learning models to synthesize information from images and clinical data. Ultimately, they execute experiments to assess the models' efficacy with and without the application of this approach. The results demonstrate an approximate 7% improvement in balanced accuracy due to the implementation of the aggregating technique. In a study [22], the authors utilized the Google Inception V4 deep learning model to evaluate the diagnoses of 58 dermatologists. The research employed a dataset consisting of medical records, dermoscopic images, and digital images from 100 subjects. The CNN outperformed most dermatologists. This study [23] presented an efficient medical image fusion model employing a deep CNN architecture for diverse multi-modal medical images obtained from both standard and real medical data. The proposed method depends on the extraction of diverse information from CT and MR images. The authors of the study [24] utilized a cloud-based model-driven architecture with deep learning algorithms to create models that improve the precision of skin cancer forecasts. The research demonstrates the methodology for constructing models and utilizing them to categorize dermal cell images. The model demonstrated better classification accuracy when comparing the results to dermatologists' diagnoses.

In another study [25], the authors trained a faster region-based convolutional neural network (FRCNN) using the training dataset and evaluated the model's performance on the test dataset. The accuracy for two-class classification (benign or malignant) is 91.5%. Another approach outlined in [26] classifies skin cancer as either melanoma or benign. The research entails segmenting skin images and extracting features to delineate the attributes of compromised skin cells utilizing a CNN model. The researchers categorized images from the ISIC 2019 dataset into eight classifications [27], and the model was trained using ResNet-50 by examining and adjusting the original parameter values using transfer learning. Images that did not conform to the established eight categories were designated as “unknown.” A study [28, 29] employed a GoogleNet pre-trained model to categorize eight varieties of melanoma. The research assessed the segmentation and performance limitations of the proposed YOLOv2-SqueezeNet in dermatology. In a study [30], the authors suggest a deep convolutional neural network (DCNN) model utilizing a deep learning approach for the precise categorization of benign

and malignant skin lesions. The authors utilized the HAM10K dataset and attained an accuracy of 91.93%.

A fully automated computer-aided diagnostic (CAD) system is offered in a study [31] based on a deep learning architecture. The suggested scheme involves the first pre-processing of original dermoscopic images using the decorrelation formulation technique, followed by lesion segmentation by MASK-RCNN. The HAM10K dataset was employed in this paper, resulting in an accuracy of 88.5%. This study [32] presents a deep learning model for the identification of skin cancer using images of skin lesions. This analytical investigation utilized 3400 images from the HAM10K dermoscopy image library. A deep convolutional neural network was created to categorize the images into benign and malignant classifications. This study attains an accuracy of 84%. The authors in a study [33] presented two distinct strategies for the automatic classification of skin diseases: (i) A standalone CNN model, and (ii) a hybrid approach combining Convolutional Neural Network with one-versus-all classification. The Convolutional Neural Network acquired a classification accuracy of 77% in detecting skin diseases across seven classes using the HAM10K dataset, whereas the integration of the Convolutional Neural Network with a one-versus-all strategy attained an accuracy of 92.90%. This work [34] employed three state-of-the-art deep learning pre-trained models, namely ResNet, Xception, and DenseNet, to categorize skin lesions. The authors utilized the HAM10K dataset for the training and evaluation of their models, achieving balanced accuracies of 78%, 82%, and 82% for the three respective models. This study [35] seeks to identify the optimal method for dermoscopy image augmentation to enhance lesion classification performance. The authors in this study devised a novel augmentation technique utilizing wavelet packet transformations where DenseNet201 deep learning model is used for training.

Table 1 demonstrates various deep-learning models historically used to classify skin cancer. Subpar performance in skin cancer classification is often attributed to insufficient or imbalanced data in the dataset. Through the studies mentioned, flaws in the suggested models were identified and addressed, indicating the potential for improving performance measures. The model's complexity was observed to contribute to longer training execution time. These tests, however, ignored how well the models performed as diagnostic tools for growing melanoma or featureless lesions. Our study uses sequential dermoscopic images and lesion change indicators to detect malignant melanomas at an early stage. Data augmentation techniques can improve accuracy by addressing dataset imbalances without modifying the model parameters. In the proposed model, accuracy increased from 86.0% to 93.43%. Comprehensive testing demonstrated that the proposed model outperforms physicians in the early detection of melanoma and surpasses other commonly used sequential models.

## 3 | Materials and Methods

### 3.1 | Dataset

We employed HAM10K dataset that was sourced from the online data portal Kaggle. After conducting fundamental preprocessing procedures, data augmentation was performed on the generated data. Data augmentation is an image processing technique that creates modified copies of the original images. Developing diverse variations of authentic images expands the dataset and enhances the generalization capabilities of deep learning models. Figure 2 illustrates the block diagram of the proposed MCADT model. For classifying skin lesions, specifically melanoma, the "Human Against Machine Melanoma" (HAM10000) dataset, listed in Table 2, is frequently used in dermatology and machine learning. 10 015 Dermoscopic images of skin lesions, including benign and malignant melanocytic lesions, are included in the HAM10000 dataset [36]. Hospitals in many nations were among the sources of these images. Relevant metadata, such as patient characteristics, lesion location, and diagnosis, are linked to each image. We have the HAM1K dataset in the form of Melanoma or not Melanoma. From here, we have grouped 7 classes into different batches to train our classifier. The Aki and Vasc classes given in Table 2 are stated as Melanoma or no Melanoma and are hence grouped into batches for training and then classifying Melanoma or Not Melanoma based on the training. The Aki and Vasc could be harmful depending on the severity of

**TABLE 1** | Literature summary.

| Paper | Size | Dataset | Algorithm | Classes | Accuracy (%) | Specificity (%) | Sensitivity (%) | F1-Score (%) |
|---|---|---|---|---|---|---|---|---|
| [30] | 300 | HAM10K | CNN | 5 | 91.43 | 96.57 | 93.66 | 95.09 |
| [28] | 1323 | HAM10K | InSiNet | 2 | 94.0.59 | — | — | — |
| [19] | 7470 | HAM10K | ResNet50 | 7 | 86.0 | 84.0 | 86.0 | 86.0 |
| [31] | 6705 | HAM10K | MASK-RCNN | 2 | 88.5 | 88.66 | 88.60 | 88.54 |
| [32] | 10 015 | HAM10K | AlexNet | 6 | 84.0 | 81.20 | 88.0 | 86.0 |
| [33] | 10 015 | HAM10K | CNN | 7 | 92.90 | 90.89 | 91.0 | 89.0 |
| [34] | 10 015 | HAM10K | DenseNet121 | 7 | 90.0 | 81.0 | 97.0 | 83.0 |
| [35] | 10 015 | HAM10K | DenseNet201 | 7 | 80.48 | 99.02 | 82.32 | 79.74 |
| Proposed | 10 015 | HAM10K | CNN | 7 | 93.43 | 88.45 | 82.05 | 85.13 |

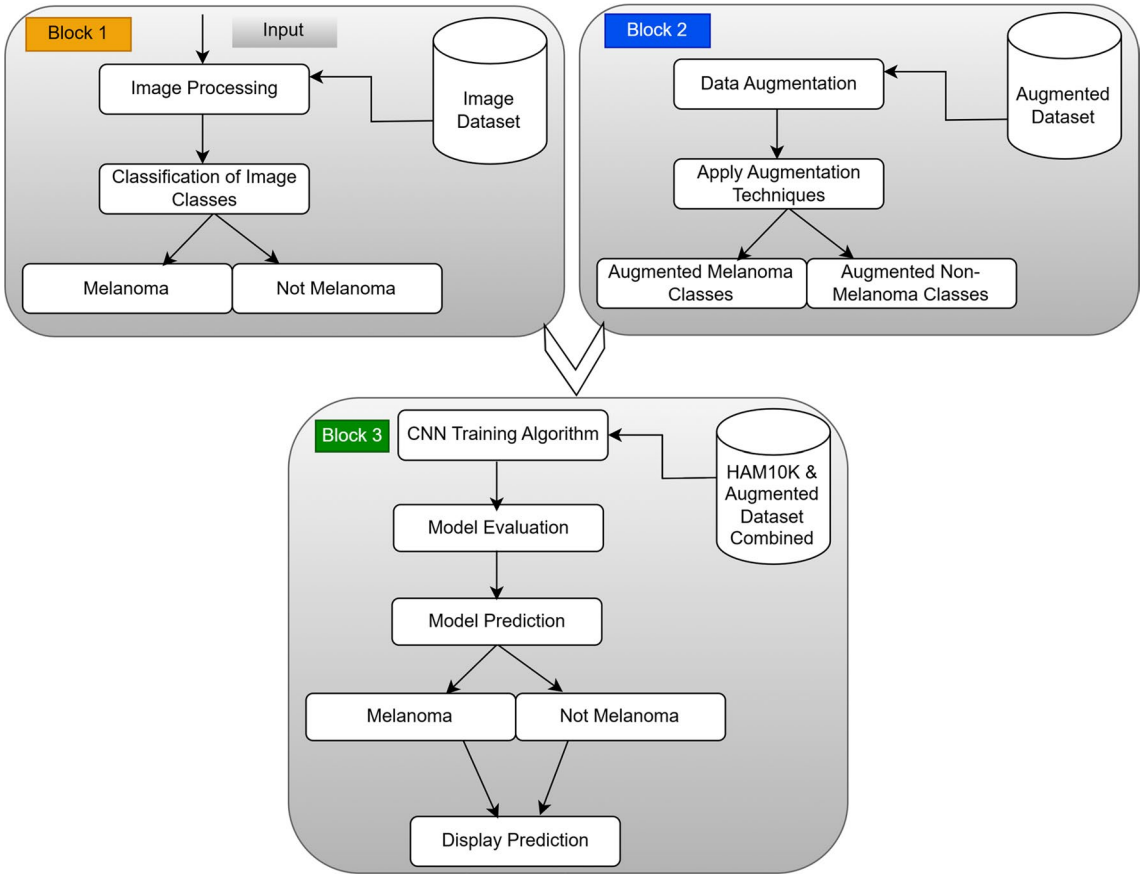


**FIGURE 2** | Proposed model block diagram.

**TABLE 2** | HAM10000 dataset.

| Class | Training images | Validation images | Testing images | Total images | Prediction |
|---|---|---|---|---|---|
| Aki | 236 | 26 | 65 | 327 | Melanoma or no melanoma |
| Bc | 371 | 41 | 102 | 514 | Melanoma |
| Bk | 792 | 88 | 219 | 1099 | No melanoma |
| Df | 72 | 8 | 35 | 115 | No melanoma |
| Mela | 802 | 89 | 222 | 1113 | Melanoma |
| Nv | 4828 | 536 | 1341 | 6705 | No melanoma |
| Vasc | 103 | 11 | 28 | 142 | Melanoma or No melanoma |

the skin in the images which could lead to the classification as Melanoma or Not Melanoma. We have divided the 10015 images dataset into training, validation, and testing by performing preprocessing steps.

In Figure 2, block 1 illustrates the image processing procedures depicted in Figure 3 that are essential for model input. Upon completion of image preprocessing, the images are placed in the image database. In block 2, we implemented data augmentation techniques, resulting in an enhanced augmented dataset stored in the augmented database. In block 3, we have integrated the Original HAM10K dataset with the enhanced dataset to train the proposed MCADT model. Upon completion of the model training, we implemented evaluation methodologies and conducted testing of the model. The model ultimately predicts whether the provided sample is melanoma or not.

### 3.2 | Pre-Processing

Data analysis and machine learning require pre-processing since the data's applicability and quality significantly impact the results and efficiency of the models. Images of melanoma skin cancer often exhibit noise due to inadequate quality, necessitating pre-processing. In a study [37], the authors detailed that during preprocessing phase, objectives include image stabilization and the minimization and refinement of noise

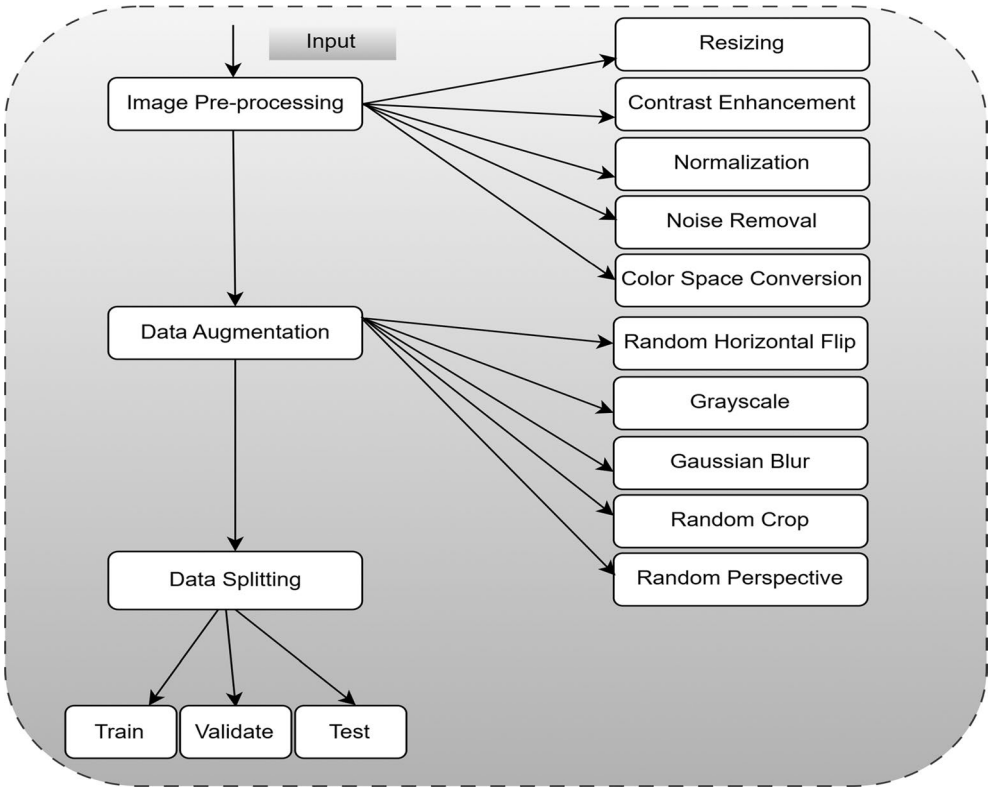


**FIGURE 3** | Overview of preprocessing.

reduction. Another study [38] discussed the importance of preprocessing. The authors explained that the influence of image preprocessing, particularly lesion segmentation, on classification accuracy has not been thoroughly investigated in numerous research. Mitigating these limitations is essential for the development of effective and practically useful skin cancer categorization systems. The pre-processing procedures used for melanoma identification are shown in Figure 3. Preprocessing establishes a uniform basis for the augmentation process. Initially, we implemented various techniques to preprocess the data. Subsequently, we employed augmentation techniques on the preprocessed data to prevent information loss during the training phase. The preprocessing approaches utilized on the HAM10K dataset are delineated below:

1. Resizing: We employed a resizing technique to alter the dimensions of the input image, ensuring uniformity across all input images.
2. Contrast Enhancement: This method was employed to augment the contrast of the input images, ensuring feature visibility and so enhancing performance.
3. Normalization: To enhance model convergence and mitigate numerical instability, we implemented normalization to scale the input images within the range [0–1].
4. Noise Reduction: Numerous factors influence the quality of images. We employed a noise reduction technique to eliminate extraneous noise from the input image.
5. Color Space Conversion: We employed a color space conversion technique to transform input images into grayscale, thereby enhancing the processing and optimizing the learning process, which subsequently improves performance.

Table 3 presents the enhanced dataset. For class Bc, we utilized the Gaussian Blur augmentation technique, resulting in 3223 augmented images, whereas for class Mela, the Random Perspective method yielded 5680 augmented images. These two classes are classified as melanoma. We acquired a total of 8903 augmented images for the melanoma category. Conversely, we implemented RandomHorizontalFlip on Aki, yielding 2830 images. We utilized Randomcrop on the Bk class, resulting in 2016 images; Random Perspective on the Df class, yielding 1650 images; Gaussian Blur on the Nv class, producing 1531 enhanced images; and Greyscale on the Vasc class, generating 875 augmented images. In the non-melanoma category, we acquired a total of 8902 augmented images. Ultimately, we partitioned the augmented images for training, validation, and testing purposes.

### 3.3 | Data Augmentation

Combining several augmentation methods can improve the performance and generalization of models. The properties of the melanoma images and the desired augmentation objectives, such as enhancing model resilience, decreasing overfitting, or broadening the training dataset, are considered while choosing the most suitable augmentation strategies [39]. 1113 images in the sample showed melanoma, while 8902 images showed skin lesions untouched by the disease. Melanoma group data was augmented in several ways to resolve the substantial data disparity. As illustrated in Figure 4, this

**TABLE 3** | Augmented dataset.

| Class | Training images | Validation images | Testing images | Augmented images | Method applied |
|---|---|---|---|---|---|
| Melanoma | | | | | |
| Bc | 2256 | 322 | 645 | 3223 | GaussianBlur |
| Mela | 3976 | 568 | 1136 | 5680 | Random perspective |
| Total | 6232 | 890 | 1781 | 8903 | — |
| Non-Melanoma | | | | | |
| Aki | 1981 | 283 | 566 | 2830 | Random horizontal flip |
| Bk | 1411 | 202 | 403 | 2016 | Random crop |
| Df | 1155 | 165 | 330 | 1650 | Random perspective |
| Nv | 1072 | 153 | 306 | 1531 | GaussianBlur |
| Vasc | 613 | 87 | 175 | 875 | Grayscale |
| Total | 6232 | 890 | 1780 | 8902 | — |

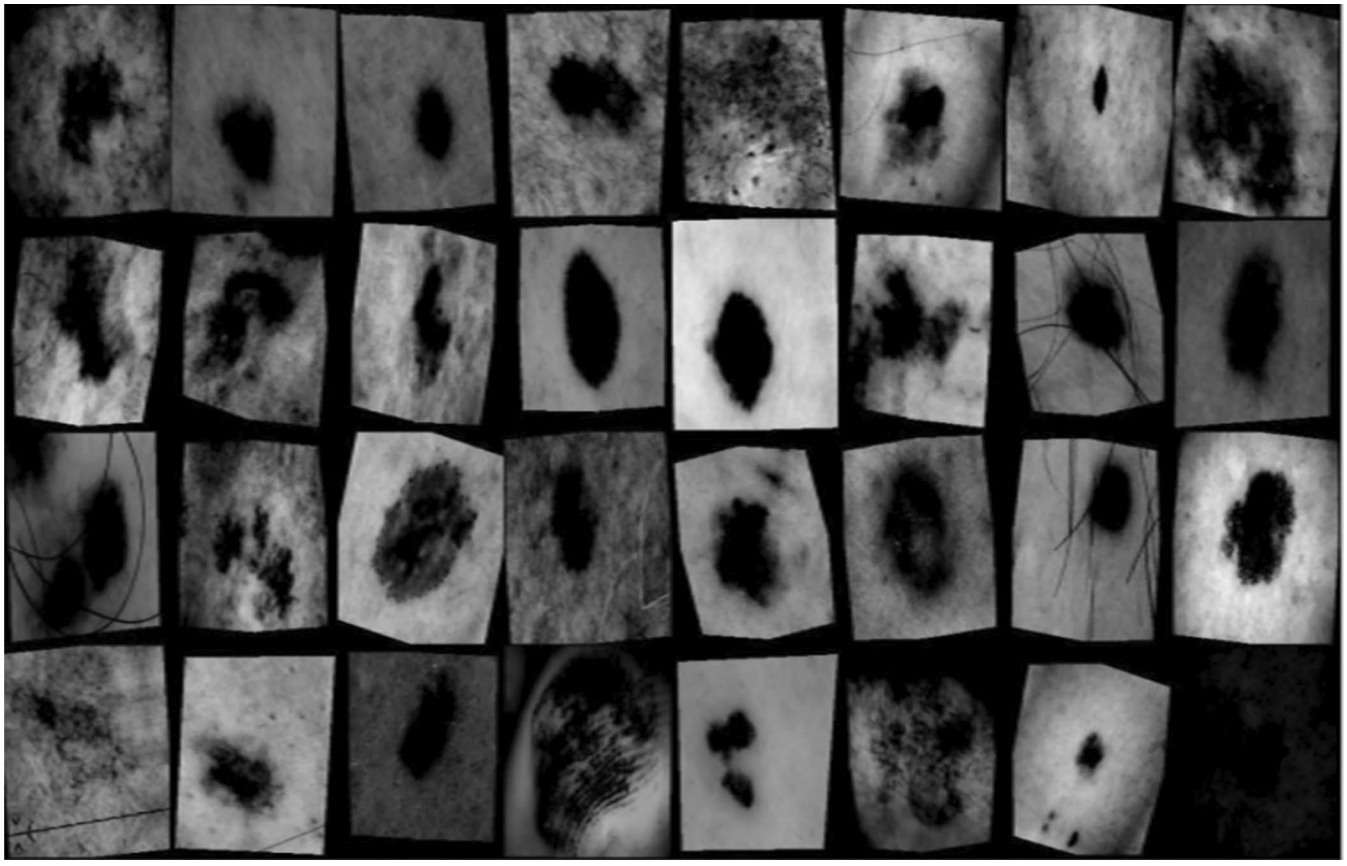

**FIGURE 4** | Augmented dataset.

procedure produced an enhanced collection of 17 805 images, split evenly between 8903 images showing melanoma and 8902 images showing various forms of skin cancer as shown in Table 3. We utilized five augmentation strategies, namely RandomHorizontalFlip, RandomCrop, RandomPerspective, GaussianBlur, and Greyscale, to improve the dataset in each class of melanoma and non-melanoma. We implemented an enhancement rule proportional to the number of samples in each category of the HAM10K dataset. Below, we provide a comprehensive explanation of each augmentation approach and the rationale for our selection of these procedures:

1. Random Horizontal Flip: It allows the model to learn from both the original image and its mirrored counterpart, providing more diverse examples for training. The model's capacity to generalize to new data is enhanced and overfitting is less likely as a result of this increased variability [40]. Without having to gather any new images, we can double

the amount of the dataset that our model was trained on. By adding variances to the data, it made the model more capable of identifying melanoma.

2. Random Crop: By applying Random Crop, the model becomes more robust to variations in image composition. Regardless of where the melanoma lesion is located in the image, it learns to focus on the pertinent region of interest (ROI) that contains it [40]. By dividing the original image into subsets, it expands the dataset. Machine learning models frequently rely on certain information found in training data. Therefore, the random crop is employed to prevent overfitting by training the model traits that are consistently present in the subsets, reducing the likelihood that it would overfit to particular details.

3. Grayscale: By converting images to grayscale, the model becomes less sensitive to color variations, allowing it to focus on texture and structural patterns. Lesions from melanoma frequently have distinctive abnormalities in texture and shape, which are particularly noticeable in grayscale [40]. The model has to learn features from three channels when working with color images; however, we transformed the images to grayscale so that the model could only learn from one channel. Our model becomes computationally efficient as a result.

4. Gaussian Blur: Real-world images can deteriorate in several ways. For instance, camera movement-induced blurring, out-of-focus effects, and so forth. To help our model learn these variations and become more resilient to these flaws, we implemented Gaussian blur. Gaussian blur applies changes while maintaining the image's overall content. By applying Gaussian blur, the model becomes less sensitive to noisy details, allowing it to focus on the underlying structure and features of the melanoma lesion [40].

5. Random Perspective: Melanoma lesions can exhibit various shapes and irregularities, resulting in geometric distortions in the images. By applying a Random Perspective, the model becomes more robust to such distortions [40]. From our perspective, everything is centered and upright in the real world. In our subset of images, RandomPerspective added distortions that made the model more versatile and able to identify objects within the image independent of the orientation or point of view. Furthermore, training the model with only precisely aligned images can cause it to become overfit, therefore we used this technique to prevent overfitting and enhance the model's performance.

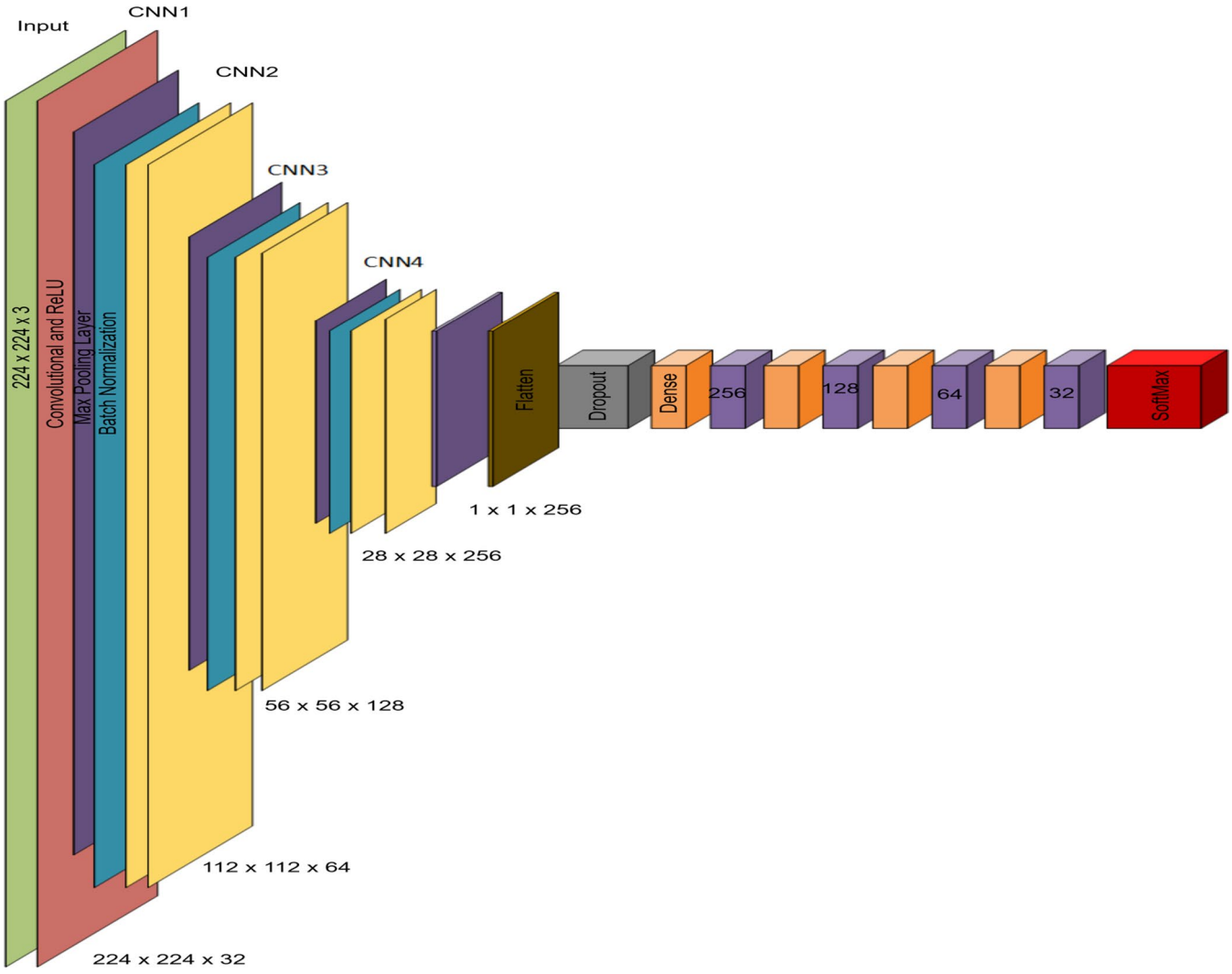


**FIGURE 5** | Proposed classification model.

### 3.4 | Proposed Model MCADT

This study aimed to categorize skin lesions using the proposed model. The dataset's images have been downsized to 224×224 pixels. The original dataset was then divided into three subsets, resulting in the creation of three separate datasets. Seventy percent, 10%, and 20% of the total images in the dataset were contained in the training, validation, and test sets. Table 2 displays a statistical breakdown of the seven distinct categories.

A convolutional neural network is a powerful deep-learning model renowned for automatically recognizing and extracting image features [38]. Its exceptional performance has made it a crucial tool in medical image analysis and other sectors. A typical convolutional neural network design consists of several layers as shown in Figure 5 [41].

Before being fed into the proposed model as input, the image pixels undergo pre-processing to prepare them appropriately. In the convolution layer of a proposed model, feature vectors also referred to as filters, are employed to extract a set of features from the original input pixels, enabling automated feature extraction [42]. Convolution, the fundamental feature of the suggested model based on a CNN, allows this procedure [43].

Using filters on an input vector, a dimensionality reduction technique is applied during the pooling process. As the filter window is dragged across the original input vector, the reduction procedure selects the minimum, maximum, or median value [44]. The outcome was a reorganization of the data file with the addition of only two new items of information: the image file path and the type of lesion. Next, the text labels for each lesion were converted into numerical values between 0 and 6. Deep learning is widely recognized as effective when dealing with large datasets. However, it is essential to note that deep learning techniques typically require significant processing time and storage resources [45]. In this research, a customized convolutional neural network model was developed for diagnosing skin lesions, as shown in Figure 6. The input images utilized have a 224×224 pixel resolution. Within each layer, the initial two sub-layers involve convolutions, where 32 filters of size 3×3 with a ReLu activation function are applied. After this, a batch normalization

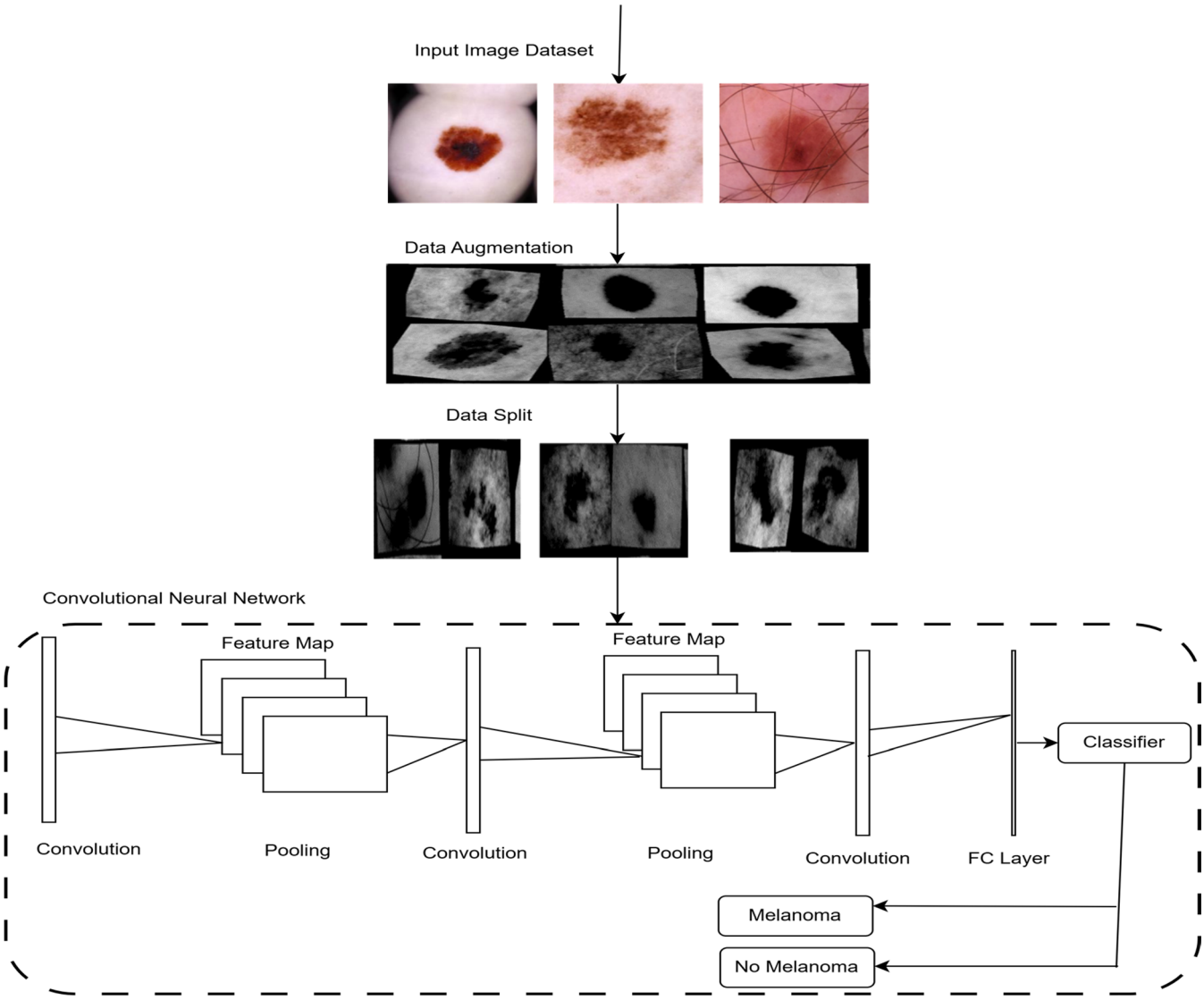


**FIGURE 6** | Proposed model architecture.

layer and a 2D max pooling layer with a 2×2 pool size come. The same convolution technique is used, but with modified parameter choices, in the second layer of the proposed model. In particular, 64×3×3 filters with a ReLu activation function are used. A 2×2 2D max pooling layer and a batch normalization layer are used after the ReLu activation. The identical convolution method is also used in the third layer but has different parameters. 128×3×3 filters with a ReLu activation function are used in this layer. Next, a 2×2 2D max pooling layer and a batch normalization layer are applied.

The suggested model's fourth layer likewise goes through a comparable convolution procedure but uses a different set of parameters. The batch normalization layer, 2D max pooling layer, dropout layer with a 20% dropout rate, and flattening layer come after this layer, which has 256 filters of size 3×3. As seen in Figure 5, the classifier receives the output from the flattening layer for the last classification stage. We used ADAM optimizer, which is a stochastic optimization algorithm. Random mini-batches of data are used by stochastic optimization methods to determine the gradient of the loss function. The operation of stochastic optimization algorithms is sequential but stochastic (random). Sequentially, the model parameters are updated iteratively in response to the data. However, they add unpredictability by estimating gradients and updating the model parameters using mini-batches or random data samples. The optimization process is strengthened and escapes local optima thanks to this stochasticity. The details of the model, including hyperparameters, can be found in Table 4.

Every one of these hyperparameters has a fixed size. The ideal values vary depending on several variables, including processing power, model complexity, and data volume. We selected the batch size, epochs, and learning rate since they were appropriate in various combinations for our model. Because there are fewer parameter adjustments per epoch when using a batch size of 32, our model trains more quickly. Although there is no set amount of epochs needed to train the model, we decided to use 50 since they were the most appropriate for our model. To improve training and performance for the specified model, we can control model changes and adjustments using the learning rate parameter. We determined that a learning rate of 0.001 would work best for our model. The optimal method for examining the range of hyperparameter values can be found by applying the Grid search or random search methodology. Setting hyperparameters is an iterative process which is used in each model. To determine which parameters would work best for the suggested model, we experimented, assessed, and improved. When compared to benign moles, melanoma is a very uncommon type of skin cancer. As a result, there is a class imbalance in the training set, with a much smaller number of benign than melanoma images. Utilizing methods such as RandomHorizontalFlip, RandomCrop, and RandomPerspective, the collection of melanoma images was manipulated unnaturally. This facilitates the model's efficient learning from the scant positive class (melanoma) data. It is possible to alter the loss function during training so that misclassified melanoma images are given higher weights. Lesions from melanoma can take on a variety of forms, dimensions, hues, and textures. Because of this heterogeneity, it may be challenging to differentiate them from benign moles using conventional procedures. For this task, we employed a customized CNN, though. By addressing the issues of class imbalance and image fluctuation, the suggested AI-powered model with CNNs has the potential to greatly increase the accuracy of melanoma identification.

**TABLE 4** | Proposed model hyper-parameters.

| Parameter | Value |
|---|---|
| Batch size | 32 |
| Epochs | 50 |
| Optimizer | Adam |
| Learning rate | 0.001 |
| Kernel size | 3 |
| Dropout | 0.4 |

## 4 | Results and Discussion

By using the classification report as shown in Table 5, the model's performance is evaluated. These four categories offer insights into accurate and inaccurate predictions regarding the correct labels, which aids in comprehending the performance and accuracy of a classification algorithm.

### 4.1 | Evaluation

The metrics for the evaluation of the proposed approach are as follows:

$$\text{Accuracy} = \frac{TP + TN}{TP + TN + FP + FN} \tag{1}$$

$$\text{Sensitivity} = \frac{TP}{TP + FN} \tag{2}$$

$$\text{Specificity} = \frac{TN}{TN + FP} \tag{3}$$

$$\text{F1} - \text{Score} = \frac{2 * (Specifity * Sensitivity)}{(Specifity + Sensitivity)} \tag{4}$$

### 4.2 | Results

After training the proposed model on the test set, predictions were made to evaluate their performance. The final layer of

**TABLE 5** | Proposed model classification report.

| | Precision | Recall | F1 Score | Support |
|---|---|---|---|---|
| 0 | 1.0 | 0.87 | 0.93 | 1781 |
| 1 | 0.89 | 1.0 | 0.94 | 1780 |
| Accuracy | — | — | 0.93 | 3561 |
| Macro AVG | 0.91 | 0.93 | 0.93 | 3561 |
| Weighted AVG | 0.94 | 0.93 | 0.93 | 3561 |

the proposed model architecture, the SoftMax layer, generated the prediction probabilities for each of the seven classes. Evaluating the models' performance is crucial to selecting the most suitable one for skin lesion classification. An analysis was conducted on the experimental data obtained from the proposed model.

Every image in the collection was scaled to a size of $224 \times 224 \times 3$ to guarantee consistency. The DL models were tested using the Tensor Flow Keras application on a machine equipped with Windows 10, 16 GB of RAM, SSD, GPU RTX3070, and Intel Xeon W1370. The proposed model was trained using a randomly selected image set that accounted for 80% of the available data. During the training process, 10% of the training data was set aside as a validation set to monitor the model's performance. The weights corresponding to the most effective combinations were kept for future use. For pre-training the suggested framework, the HAM10000 dataset was utilized. The framework employed the Adam optimizer, a popular optimization algorithm in deep learning. Additionally, a learning rate technique was implemented to slow down the learning process when there was no significant improvement in performance over an extended period (referred to as validation patience). The training process incorporated specific hyperparameters for the Adam optimizer, including a batch size of 32 and 50 epochs. A technique called "batching" was employed to enhance anti-ineffective measures, which involves dividing the training data into smaller batches for processing.

### 4.3 | Discussion

The findings in Table 6 and Figure 7 show that our technique performs better than others in efficiency and effectiveness. In particular, the proposed model outperforms current techniques with an excellent accuracy rate of 93.43%. Metrics, that is, sensitivity and specificity, are frequently employed to assess the effectiveness of binary classification models in the medical field, including those for melanoma. Each indicator has advantages and disadvantages and offers various insights into the model's performance. Our model correctly identified 93.43% of the samples, indicating an accuracy of 93.43%. With a 99.74% sensitivity, the model almost always accurately predicts melanoma. The performance improvement is because the proposed classifier automatically learns hierarchical features from images.

The structure comprises several layers with adjustable filters, enabling the extraction of low-level features such as edges and textures in the initial levels, while progressively developing high-level features like object components and intricate shapes in the deeper layers. This hierarchical feature learning is crucial for image categorization as it facilitates the capture of both local and global trends. Furthermore, the proposed classifier possesses intrinsic translation invariance owing to its convolutional layers. This indicates their ability to identify patterns irrespective of their precise location within an image. In image classification, the exact location of an object within the image

**TABLE 6** | MCADT confusion matrix.

| True positive | False negative | False positive | True negative |
|---|---|---|---|
| 1551 | 4 | 230 | 1776 |

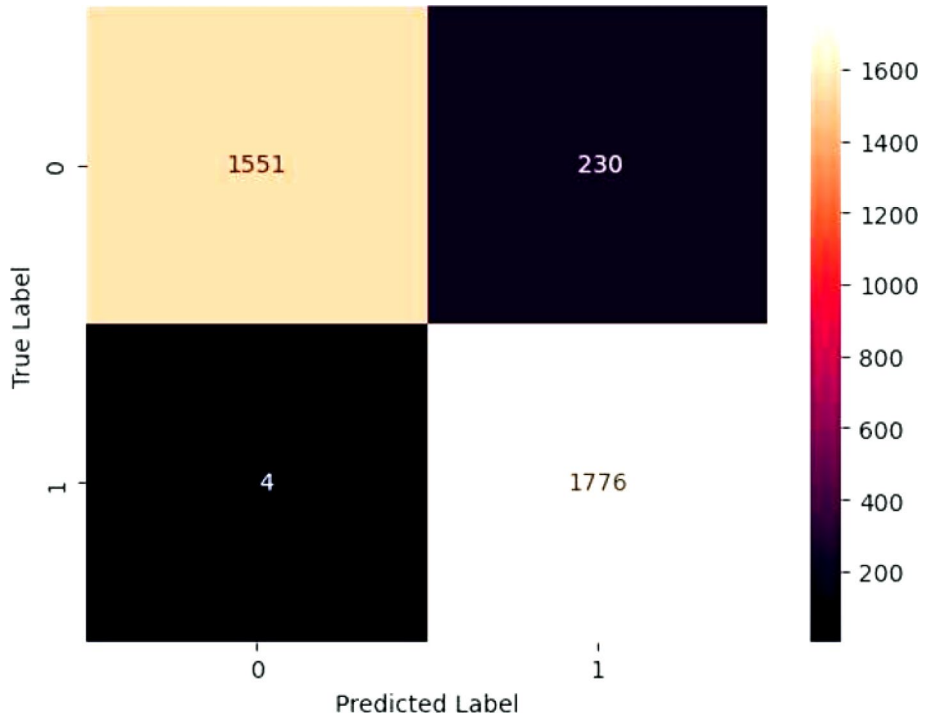


**FIGURE 7** | MCADT model confusion matrix.

**TABLE 7** | Comparison of the proposed approach with SOTA methods.

| Paper | Dataset | Model | Accuracy (%) | Specificity (%) | Sensitivity (%) | F1- Score (%) |
|---|---|---|---|---|---|---|
| [30] | HAM10K | CNN | 91.43 | 96.57 | 93.66 | 95.09 |
| [32] | HAM10K | AlexNet | 84.00 | 81.20 | 88.0 | 86.0 |
| [33] | HAM10K | CNN & ResNet | 92.90 | 90.89 | 91.0 | 89.0 |
| [34] | HAM10K | DenseNet121 | 90.0 | 81.0 | 97.0 | 83.0 |
| [18] | HAM10K | CNN and ResNet-50 | 86.00 | 67.81 | 75.83 | 71.60 |
| [15] | HAM10K | G-DMN MobileNetV2 | 87.07 | 76.30 | 77.49 | 76.89 |
| [35] | HAM10K | DenseNet201 | 80.48 | 99.02 | 82.32 | 79.74 |
| [46] | HAM10K | CNN variants | 90 | 88.06 | 80.66 | 83.77 |
| **Proposed** | **HAM10K** | **Proposed approach** | **93.43** | **88.45** | **82.05** | **85.13** |

should not influence the model's capacity for recognition, and CNNs are particularly adept at this task. The convolutional procedure in CNNs decreases the parameter count and, hence, the likelihood of overfitting. It also aids in maintaining the spatial relationships among pixels, which is essential for image categorization tasks. The proposed model outperformed SOTA models in comparison as it is shown in Table 7.

### 4.4 | Ablation Study

The ablative analysis seeks to determine the superior categorization by examining the iteration-based performance of the models in relation to the performance indicators. Ablation studies were undertaken inside the methodology to assess the influence of several components, such as batch size, optimizer, number of epochs, and learning rate, on the overall performance of the proposed system. In the ablation investigations, we emphasized the significance of the image augmentation and identification of region of interest, as it is executed via the CNN model to provide precise segmented masks, hence preventing false detections by isolating pertinent areas for examination. A comparison analysis has been conducted to identify the effects of the different settings in the suggested methodology. Figures 8 and 9 presents the assessment of the suggested method both with and without setting hyperparameters. The findings indicated that each component is essential for improving model performance and significantly influences the detection of melanoma skin cancer, yielding superior outcomes.

To assess the efficacy of the proposed method for skin cancer prediction, we utilized the pertinent publically available dataset, HAM10K. We implemented image augmentation and improved the dataset. We own a total of 10 015 original images and 17 805 augmented images, resulting in 27 820 images overall. We have utilized melanoma images to evaluate the efficacy of the proposed methodology.

Figure 10 displays the samples of the melanoma images. The efficacy of the suggested method on novel testing data derived from the customized dataset is nearly uniform, as evidenced by the achieved accuracy of 93.43%, suggesting that the proposed

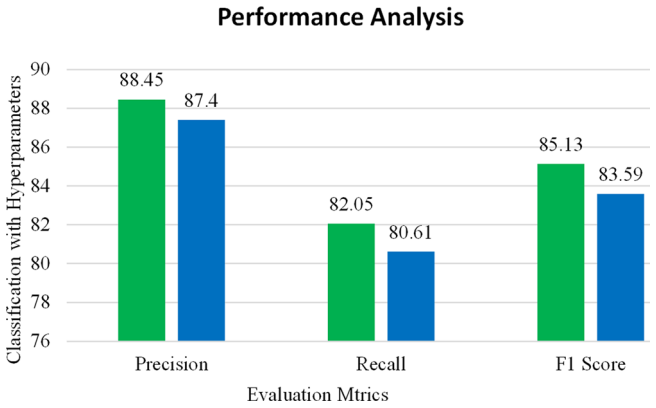


**FIGURE 8** | Performance evaluation with best hyperparameters settings.

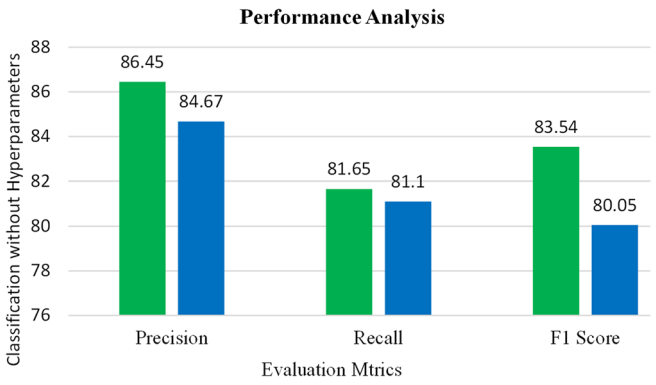


**FIGURE 9** | Performance evaluation with fine-tuning hyperparameters.

system applies to datasets of diverse sizes without considerable effect on performance.

The findings of the ablation study on the improved and HAM10K datasets are presented in Table 8. The results demonstrate the impact of various hyperparameters. The image size remained unchanged as it was maintained at the initial settings. The aim was to thoroughly investigate various hyperparameters to evaluate their impact on the model's generalization

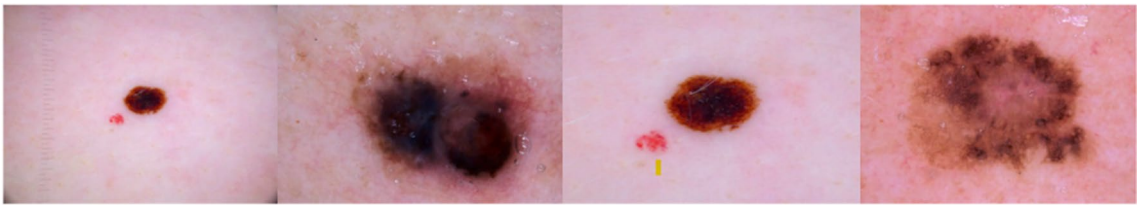

**FIGURE 10** | Melanoma samples from HAM10K dataset.

**TABLE 8** | Performance evaluation with different hyperparameters.

| Hyperparameter | Function applied | Accuracy (%) | Precision (%) | Recall (%) | F1- Score (%) |
|---|---|---|---|---|---|
| Activation function | Sigmoid, ReLu | 89.31 | 88.37 | 88.31 | 87.13 |
| Augmentation | Yes | 93.43 | 88.45 | 82.05 | 85.13 |
| | No | 89.33 | 87.55 | 87.15 | 86.83 |
| Pooling layer | Average and max-pooling | 85.52 | 84.44 | 84.24 | 83.42 |
| Padding | 1, 2 | 83.80 | 82.90 | 82.50 | 81.00 |
| Kernel size | 3×3 and 5×5 | 86.05 | 87.10 | 86.05 | 84.50 |
| Loss function | Binary and cross entropy | 88.20 | 86.75 | 84.50 | 82.65 |
| Batch size | 32, 64, 128, and 256 | 82.70 | 76.30 | 80.30 | 79.20 |
| Optimizer | Adam and RMSprop | 84.51 | 85.20 | 84.28 | 81.81 |
| Learning rate | 0.001, 0.003, 0.004, and 0.006 | 89.12 | 88.61 | 87.91 | 85.19 |
| # of epochs | 20, 40,50, and 60 | 91.09 | 90.46 | 89.64 | 88.71 |

ability. We executed our model utilizing two activation functions: Sigmoid and ReLU. We experimented with many configurations for these two activation functions and selected the optimal one, which is ReLU. In the subsequent phase, we evaluated our model both with and without augmentation, discovering that the implementation with augmentation yielded more favorable results, achieving an accuracy of 93.43%. The research demonstrates that the feature conversion approach is the most critical among the assessed characteristics. In the conversion of 2D future maps into 1D feature vectors, global max pooling exhibits superior performance across datasets, while global average pooling shows inferior performance. Subsequently, we implemented padding of 1 and 2, along with kernel sizes of 3×3 and 5×5. We determined that the optimal configuration was a padding of 1 and a kernel size of 3×3, which yielded an accuracy of 93.43% for our model. We utilized cross entropy and binary cross entropy to assess our model under various configurations, ultimately selecting cross entropy as our loss function. The reduced batch size of the model led to a slight decrease in accuracy, underscoring its effectiveness in determining the optimal model state. Consequently, we selected batch sizes of 32, 64, 128, and 256 in the initial configurations and did not alter this parameter, as it yielded the best results when assessing the performance of our MCADT model. Nonetheless, the optimizer, stride size variations, and the number of epochs rank among the least consequential hyperparameters. In the HAM10K dataset, Adam exhibited superior performance, exceeding RSMprop, which achieved the lowest accuracy. The learning rate has been a crucial hyperparameter in this experiment.

A learning rate of 0.006 led to an overfitted model; however, a gradual reduction in the learning rate significantly improved accuracy. We conducted more tests using learning rates of 0.001, 0.003, and 0.004; however, we determined that a learning rate of 0.001 was optimal for our model, and thus we proceeded with further experiments at this rate. Ultimately, we tested our model with varying numbers of epochs to assess its efficacy. We utilized epochs of 20, 40, 50, and 60, determining that 50 yielded the optimal accuracy of 93.43%, leading to its selection as the preferred epoch count. This study indicates that peak performance occurs at 50 epochs, beyond which accuracy starts to diminish. We trained our MCADT model with the hyperparameters specified in Table 8. This configuration, as outlined by the ablation study, determines the optimal combination for achieving superior performance results. The reduction of convolutional layers and the elimination of dropout layers dramatically impaired the model's capacity to generalize and comprehend intricate patterns, evidenced by a decline in accuracy and other performance indicators. We conducted a comparison analysis utilizing assessment criteria including precision, recall, and the F1 score to independently assess performance in the binary categorization of malignant versus benign. The ablation study offers essential insights into the interrelationships and significance of each model component and training approach, confirming their combined impact on classification accuracy and robustness in real-world applications. Table 8 presents the ablation study, emphasizing the impact of various model configurations and training strategies on performance indicators. The results indicate that this method enhanced performance for benign lesions,

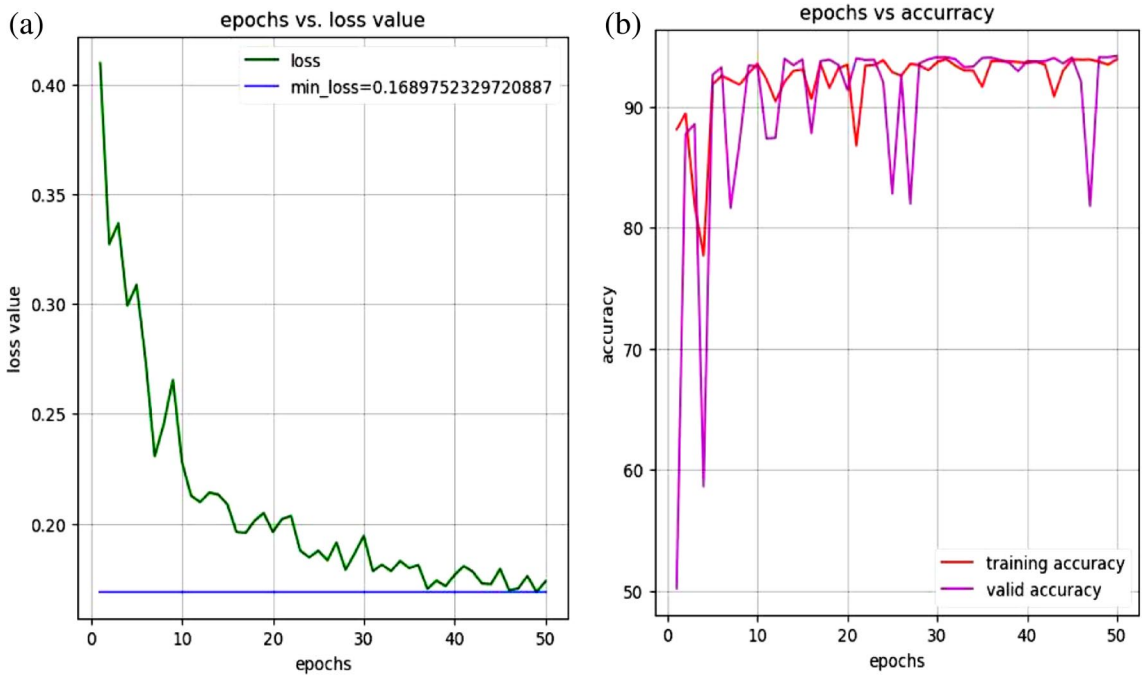


**FIGURE 11** | (a). MCADT model Loss, (b). MCADT model accuracy.

attaining 82.05% precision, 88.45% recall, 85.13% F1 score, and 93.43% accuracy.

### 4.5 | Knowledge Gap and Potential Solution

Treatments for melanoma, a deadly form of skin cancer, are successful if caught in time. In this study, we attempted to apply a CNN-based model that can significantly outperform traditional methods in terms of melanoma detection speed and accuracy. This will enable the machine to evaluate skin scans with consistency and a level of detail that may be challenging for human clinicians to achieve. First, we see the knowledge gap in the dataset, where the acquisition of diverse and high-quality datasets for AI model training is one of the main obstacles. A lot of the datasets that are now available are not large enough to accurately reflect the variety of skin types, melanoma subtypes, and lesion features. To bridge this gap, researcher specialists work with healthcare organizations to have access to sizable and varied datasets. Additionally, data augmentation methods are being used to improve the caliber and diversity of training data as in this study. We see there are difficulties in incorporating AI-based melanoma diagnosis into clinical practice, even despite the technology's encouraging outcomes in research settings. AI system adoption may be resisted by healthcare practitioners because of worries about workflow integration, liability, and dependability. To allay these worries and guarantee that artificial intelligence (AI) systems adhere to privacy, safety, and efficacy regulations, researchers collaborate closely with regulators and physicians. The application of AI to melanoma diagnosis presents significant ethical and societal issues about patient privacy, consent, and equity.

These issues are addressed by considering responsibility and collaborating with stakeholders, such as patients, healthcare practitioners, policymakers, and ethicists. Since more and more AI-powered melanoma diagnostics are being used in clinical settings, the field of improving melanoma diagnostics is expected to see substantial breakthroughs and changes over the next five years. Additional AI algorithms will examine multimodal data, such as clinical results, histological pictures, and genetic profiles, to clarify the molecular pathways underlying the development of melanoma and find novel targets for therapeutic intervention. Based on the loss plots, error rate, and validation accuracy for each model, we discovered that although the loss decreased as shown in Figure 11a, accuracy increased as shown in Figure 11b, indicating no signs of overfitting.

### 4.6 | Limitations and Future Perspective of MCADT

To enhance the small number of datasets available in our model, we gathered the HAM10K dataset and used techniques for data augmentation such as random crop. To divide the dataset into training, validation, and testing phases, we carried out preprocessing procedures. We selected CNN as our foundational model and optimized its internal structure to better fit our model's needs. To prevent overfitting and manage fluctuations, we fine-tuned the hyperparameters of the model. We assessed the performance of our model using metrics from classification reports, such as sensitivity, accuracy, and so forth. We used software libraries like TensorFlow and hardware GPUs with the specs already listed in the article. We choose CNN because, in comparison to other algorithms, it offers more learning capacity, scalability, and adaptability in the diagnosis of melanoma and is robust in image processing. Their capacity to identify complex patterns from large volumes of data is essential for a precise and trustworthy diagnosis of melanoma. A dataset that is trained using CNN may be skewed toward a specific kind of lesion. The model may not perform well if the information was gathered from a single source clinic since the

lesion identifications may not be as diverse as they are in real-world situations. When a model is trained on a limited collection of datasets, it may not function effectively on unobserved data with distinct features, such as camera movement. Due to its intricate architecture or small dataset, this type of model may overfit, which can deteriorate performance when tested on untested data. The following are some possible effects of the suggested model on patient care:

1. Effective treatment depends on early detection. Our CNN model could be useful in diagnosing melanoma early on and in treating it before it worsens.
2. By evaluating images and emphasizing lesion regions, our suggested model can assist dermatologists in improving the diagnostic procedure.
3. We will help and benefit rural locations without access to specialized dermatologists by implementing our suggested model.
4. Our approach can lower expensive medical bills and laboratory testing costs.
5. Patients would be self-aware of their health and able to track changes in their skin to identify melanoma early on.

## 5 | Conclusion

A common condition, skin cancer, can be initially detected visually and verified by dermoscopic analysis and other procedures. Computer-assisted models are becoming increasingly crucial due to a shortage of competent specialists and efforts to lower human error. A deep learning technique for image analysis, known as a convolutional neural network, has been successful in computer vision. This study created a method to examine skin lesions and rapidly and precisely diagnose seven types of skin cancer. This study enhances lesion images to increase visibility and decrease noise. This study uses pre-processed medical pictures of skin lesions from the HAM10K dataset to train the proposed model to decrease overfitting and enhance the overall performance of the suggested deep-learning techniques. With a sensitivity of 82.05% and a specificity of 88.45%, the presented model demonstrated an incredible accuracy rate of 93.43%, which is on par with the accuracy of dermatologists with professional training. Using data augmentation as a pre-processing step, the research contributed a novel contribution to the area. This step helped the suggested model perform better than pre-trained models already in use. The proposed model outperformed SOTA models in comparison. The proposed work has the potential to save time and improve precision in the diagnosis of skin cancer, benefiting both patients and healthcare professionals. This study performed well on the detection of melanoma using the HAM10K dataset with augmentation, however, we could not perform it on other datasets.

### 5.1 | Future Directions

In the future, we aim to focus on real-time diagnosis of skin lesions and improve the testing accuracy of their model. Dermatologists will be able to assess and categorize skin cancer classes more precisely and effectively, which will also aid in enhancing performance metric scores. In the future, we plan to experiment with our model on other available skin cancer datasets that could enhance the accuracy of diagnosing melanoma patients. Furthermore, with the assistance of several hospitals and keeping in mind the confidentiality of patient information, we will consider incorporating other data modalities, like genetic information, clinical history, patient demographics, and dermoscopic images. Combining data from several sources may improve the accuracy and resilience of melanoma classification. For dermatologists, real-time diagnosis will improve workflow efficiency. Implementing future directions requires faster processing requirements. To help dermatologists have confidence in the model's decision-making process, explainable AI techniques will be integrated into the models. The model's training process involves sensitive patient data, so data security is a critical precaution that must be taken. Data privacy laws, such as HIPPA, would guarantee adherence to the necessary rules. Our continued efforts should be able to lower the death rate and create a more robust society. Additionally, it would lessen the strain on healthcare systems. It would assist individuals dealing with melanoma in reducing their fear and anxiety. Maintaining a healthy lifestyle would be much easier with real-time diagnosis. In the future, we also aim to perform model training and testing with ISIC versions of datasets to further strengthen our model's robustness and hence the performance in accurately detection of skin lesions whether they are melanoma or non-melanoma.

#### Author Contributions

Conceptualization, M.S. A.H.K. and T.S.M.; methodology, M.S. A.H.K. and T.S.M.; software, A.B. and Z.A.; validation, M.S. A.H.K. and T.S.M.; formal analysis, A.B. and Z.A.; investigation, R.S.; resources, R.S.; data curation, A.B. and Z.A.; writing – original draft preparation, M.S.; writing – review and editing, A.B. and Z.A. funding acquisition, R.S. All authors have read and agreed to the published version of the manuscript.

#### Conflicts of Interest

The authors declare no conflicts of interest.

#### Data Availability Statement

Data sharing not applicable to this article as no datasets were generated or analysed during the current study.

#### References

1. A. Patel, "Benign vs Malignant Tumors," *JAMA Oncology* 6, no. 9 (2020): 1488, https://doi.org/10.1001/jamaoncol.2020.2592.

2. T. Saba, "Computer Vision for Microscopic Skin Cancer Diagnosis Using Handcrafted and Non-Handcrafted Features," *Microscopy Research and Technique* 84, no. 6 (2021): 1272–1283, https://doi.org/10.1002/jemt.23686.

3. A. Rizzo, V. Mollica, V. Tateo, et al., "Hypertransaminasemia in Cancer Patients Receiving Immunotherapy and Immune-Based Combinations: The Mouseion-05 Study," *Cancer Immunology, Immunotherapy* 72, no. 6 (2023): 1381–1394, https://doi.org/10.1007/s00262-023-03366-x.

4. M. A. Khan, M. I. Sharif, M. Raza, A. Anjum, T. Saba, and S. Ali Shad, "Skin Lesion Segmentation and Classification: A Unified Framework of Deep Neural Network Features Fusion and Selection," *Expert Systems* 39, no. 7 (2019): e12497, https://doi.org/10.1111/exsy.12497.

5. M. A. Khan, M. Sharif, T. Akram, R. Damaševičius, and R. Maskeliūnas, "Skin Lesion Segmentation and Multiclass Classification Using Deep Learning Features and Improved Moth Flame Optimization," *Diagnostics* 11, no. 5 (2021): 811, https://doi.org/10.3390/diagnostics11050811.

6. V. Mollica, A. Rizzo, A. Marchetti, et al., "The Impact of ECOG Performance Status on the Efficacy of Immunotherapy and Immune-Based Combinations in Cancer Patients: The Mouseion-06 Study," *Clinical and Experimental Medicine* 23, no. 8 (2023): 5039–5049, https://doi.org/10.1007/s10238-023-01159-1.

7. F. Bray, J. Ferlay, I. Soerjomataram, R. L. Siegel, L. A. Torre, and A. Jemal, "Global Cancer Statistics 2018: Globocan Estimates of Incidence and Mortality Worldwide for 36 Cancers in 185 Countries," *CA: a Cancer Journal for Clinicians* 68, no. 6 (2018): 394–424, https://doi.org/10.3322/caac.21492.

8. I. U. Khan, N. Aslam, T. Anwar, et al., "Remote Diagnosis and Triaging Model for Skin Cancer Using EfficientNet and Extreme Gradient Boosting," *Complexity* 2021 (2021): 1–13, https://doi.org/10.1155/2021/5591614.

9. V. De Giorgi, E. Trez, C. Salvini, et al., "Dermoscopy in Black People," *British Journal of Dermatology* 155, no. 4 (2006): 695–699, https://doi.org/10.1111/j.1365-2133.2006.07415.x.

10. O. O. Kushimo, A. O. Salau, O. J. Adeleke, and D. S. Olaoye, "Deep Learning Model to Improve Melanoma Detection in People of Color," *Arab Journal of Basic and Applied Sciences* 30, no. 1 (2023): 92–102, https://doi.org/10.1080/25765299.2023.2170066.

11. K. Mahendraraj, K. Sidhu, C. S. M. Lau, G. J. McRoy, R. S. Chamberlain, and F. O. Smith, "Malignant Melanoma in African–Americans," *Medicine* 96, no. 15 (2017): e6258, https://doi.org/10.1097/md.0000000000006258.

12. T. J. Brinker, A. Hekler, A. H. Enk, et al., "Deep Neural Networks Are Superior to Dermatologists in Melanoma Image Classification," *European Journal of Cancer* 119 (2019): 11–17, https://doi.org/10.1016/j.ejca.2019.05.023.

13. I. Abunadi, "Deep and Hybrid Learning of MRI Diagnosis for Early Detection of the Progression Stages in Alzheimer's Disease," *Connection Science* 34, no. 1 (2022): 2395–2430.

14. J. Kawahara, S. Daneshvar, G. Argenziano, and G. Hamarneh, "Seven-Point Checklist and Skin Lesion Classification Using Multi-Task Multimodal Neural Nets," *IEEE Journal of Biomedical and Health Informatics* 23, no. 2 (2019): 538–546, https://doi.org/10.1109/jbhi.2018.2824327.

15. H. Wang, Q. Qi, W. Sun, X. Li, B. Dong, and C. Yao, "Classification of Skin Lesions With Generative Adversarial Networks and Improved mobilenetv2," *International Journal of Imaging Systems and Technology* 33 (2023): 1561–1576, https://doi.org/10.1002/ima.22880.

16. GSMA, "Ericsson, On the Pulse of the Networked Society, Tech. Rep," (2013).

17. APO, "Analysis & Policy Observatory," (2015), https://apo.org.au/node/59109.

18. K. Lenc and A. Vedaldi, "Understanding Image Representations by Measuring Their Equivariance and Equivalence," *International Journal of Computer Vision* 127, no. 5 (2018): 456–476, https://doi.org/10.1007/s11263-018-1098-y.

19. G. Alwakid, W. Gouda, M. Humayun, and N. U. Sama, "Melanoma Detection Using Deep Learning-Based Classifications," *Health* 10, no. 12 (2022): 2481, https://doi.org/10.3390/healthcare10122481.

20. M. Efimenko, A. Ignatev, and K. Koshechkin, "Review of Medical Image Recognition Technologies to Detect Melanomas Using Neural Networks," *BMC Bioinformatics* 21, no. S11 (2020): 270, https://doi.org/10.1186/s12859-020-03615-1.

21. G. C. Pacheco and R. A. Krohling, "The Impact of Patient Clinical Information on Automated Skin Cancer Detection," *Computers in Biology and Medicine* 116 (2020): 103545, https://doi.org/10.1016/j.compbiomed.2019.103545.

22. H. A. Haenssle, C. Fink, R. Schneiderbauer, et al., "Man Against Machine: Diagnostic Performance of a Deep Learning Convolutional Neural Network for Dermoscopic Melanoma Recognition in Comparison to 58 Dermatologists," *Annals of Oncology* 29, no. 8 (2018): 1836–1842, https://doi.org/10.1093/annonc/mdy166.

23. W. El-Shafai, N. El-Hag, A. Sedik, et al., "An Efficient Medical Image Deep Fusion Model Based on Convolutional Neural Networks," *Computers, Materials and Continua* 74, no. 2 (2023): 2905–2925.

24. M. A. Kadampur and S. Al Riyaee, "Skin Cancer Detection: Applying a Deep Learning Based Model Driven Architecture in the Cloud for Classifying Dermal Cell Images," *Informatics in Medicine Unlocked* 18 (2020): 100282, https://doi.org/10.1016/j.imu.2019.100282.

25. S. Jinnai, N. Yamazaki, Y. Hirano, Y. Sugawara, Y. Ohe, and R. Hamamoto, "The Development of a Skin Cancer Classification System for Pigmented Skin Lesions Using Deep Learning," *Biomolecules* 10, no. 8 (2020): 1123, https://doi.org/10.3390/biom10081123.

26. M. A. Kassem, K. M. Hosny, and M. M. Fouad, "Skin Lesions Classification Into Eight Classes for ISIC 2019 Using Deep Convolutional Neural Network and Transfer Learning," *IEEE Access* 8 (2020): 114822–114832, https://doi.org/10.1109/access.2020.3003890.

27. A. Hekler, J. S. Utikal, A. H. Enk, et al., "Superior Skin Cancer Classification by the Combination of Human and Artificial Intelligence," *European Journal of Cancer* 120 (2019): 114–121, https://doi.org/10.1016/j.ejca.2019.07.019.

28. H. C. Reis, V. Turk, K. Khoshelham, and S. Kaya, "InSiNet: A Deep Convolutional Approach to Skin Cancer Detection and Segmentation," *Medical & Biological Engineering & Computing* 60, no. 3 (2022): 643–662, https://doi.org/10.1007/s11517-021-02473-0.

29. Z. Lee and A. P. P. Abdul Majeed, "Classification of Skin Cancer Using Transfer Learning Models," *MEKATRONIKA* 3, no. 2 (2021): 77–81, https://doi.org/10.15282/mekatronika.v3i2.7393.

30. S. Ali, M. S. Miah, J. Haque, M. M. Rahman, and M. K. Islam, "An Enhanced Technique of Skin Cancer Classification Using a Deep Convolutional Neural Network With Transfer Learning Models," *Machine Learning with Applications* 5 (2021): 100036, https://doi.org/10.1016/j.mlwa.2021.100036.

31. T. Khan, Y.-D. Z. Akram, and M. Sharif, "Attributes-Based Skin Lesion Detection and Recognition: A Mask RCNN and Transfer Learning-Based Deep Learning Framework," *Pattern Recognition Letters* 143 (2021): 58–66, https://doi.org/10.1016/j.patrec.2020.12.015.

32. A. Ameri, "A Deep Learning Approach to Skin Cancer Detection in Dermoscopy Images," *Journal of Biomedical Physics & Engineering* 10 (2020): 801.

33. K. Polat and K. O. Koc, "Detection of Skin Diseases From Dermoscopy Image Using the Combination of Convolutional Neural Network and One-Versus-All," *Journal of Artificial Intelligence and Systems* 2 (2020): 80–97.

34. Z. Rahman and A. M. Ami, "A Transfer Learning Based Approach for Skin Lesion Classification From Imbalanced Data," in *Proceedings of the 2020 11th International Conference on Electrical and Computer Engineering (ICECE)* (Dhaka, Bangladesh: IEEE, 2020).

35. E. Goceri, "Comparison of the Impacts of Dermoscopy Image Augmentation Methods on Skin Cancer Classification and a New Augmentation Method With Wavelet Packets," *International Journal of Imaging Systems and Technology* 33, no. 5 (2023): 1727–1744, https://doi.org/10.1002/ima.22890.

36. K. M. Fouad, M. M. Ismail, A. T. Azar, and M. M. Arafa, "Advanced Methods for Missing Values Imputation Based on Similarity Learning," *PeerJ Computer Science* 1, no. 1 (2021): 1–38.

37. M. S. A. Abed and A. Akbas, "An Approach in Melanoma Skin Cancer Segmentation With Bat Optimization Algorithm," *International*

*Journal of Imaging Systems and Technology* 34, no. 4 (2024): e23119, https://doi.org/10.1002/ima.23119.

38. A. N. Toprak and I. Aruk, "A Hybrid Convolutional Neural Network Model for the Classification of Multi-Class Skin Cancer," *International Journal of Imaging Systems and Technology* 34, no. 5 (2024): e23180, https://doi.org/10.1002/ima.23180.

39. I. Iqbal, M. Younus, K. Walayat, M. U. Kakar, and J. Ma, "Automated Multi-Class Classification of Skin Lesions Through Deep Convolutional Neural Network With Dermoscopic Images," *Computerized Medical Imaging and Graphics* 88 (2021): 101843, https://doi.org/10.1016/j.compmedimag.2020.101843.

40. "Transforming and augmenting images, Transforming and augmenting images - Torchvision main documentation," accessed May 20, 2023, https://pytorch.org/vision/main/transforms.html.

41. M. S. Naeem, A. K. Farooq, and A. Abid, "Malignant Melanoma Classification Using Deep Learning: Datasets, Performance Measurements, Challenges and Opportunities," *IEEE Access* 8 (2020): 110575–110597, https://doi.org/10.1109/access.2020.3001507.

42. Z. Hu, J. Tang, Z. Wang, K. Zhang, L. Zhang, and Q. Sun, "Deep Learning for Image-Based Cancer Detection and Diagnosis A Survey," *Pattern Recognition* 83 (2018): 134–149, https://doi.org/10.1016/j.patcog.2018.05.014.

43. A. T. Azar, Z. I. Khan, S. U. Amin, and K. M. Fouad, "Hybrid Global Optimization Algorithm for Feature Selection," *Computers, Materials and Continua* 74, no. 1 (2023): 2021–2037.

44. O. Sevli, "A Deep Convolutional Neural Network-Based Pigmented Skin Lesion Classification Application and Experts Evaluation," *Neural Computing and Applications* 33, no. 18 (2021): 12039–12050, https://doi.org/10.1007/s00521-021-05929-4.

45. R. Sarkar, C. C. Chatterjee, and A. Hazra, "Diagnosis of Melanoma From Dermoscopic Images Using a Deep Depth Wise Separable Residual Convolutional Network," *IET Image Processing* 13, no. 12 (2019): 2130–2142, https://doi.org/10.1049/iet-ipr.2018.6669.

46. A. Al-Rasheed, A. Ksibi, M. Ayadi, A. I. A. Alzahrani, M. Zakariah, and N. Ali Hakami, "An Ensemble of Transfer Learning Models for the Prediction of Skin Cancers With Conditional Generative Adversarial Networks," *Diagnostics* 12, no. 12 (2022): 3145, https://doi.org/10.3390/diagnostics12123145.